



HAL
open science

Comparison of Two Fast Pressure Sensitive Paints: Measurements of an Oscillating Shock in a Transonic Flow

Walter Beck, Christian Klein, Ulrich Henne, Marie-Claire Merienne, Yves Le
Sant, Pascal Molton

► **To cite this version:**

Walter Beck, Christian Klein, Ulrich Henne, Marie-Claire Merienne, Yves Le Sant, et al.. Comparison of Two Fast Pressure Sensitive Paints: Measurements of an Oscillating Shock in a Transonic Flow. AIAA AVIATION 2018, Jun 2018, Atlanta, United States. 10.2514/6.2018-3316 . hal-04472875

HAL Id: hal-04472875

<https://hal.science/hal-04472875v1>

Submitted on 22 Feb 2024

HAL is a multi-disciplinary open access archive for the deposit and dissemination of scientific research documents, whether they are published or not. The documents may come from teaching and research institutions in France or abroad, or from public or private research centers.

L'archive ouverte pluridisciplinaire **HAL**, est destinée au dépôt et à la diffusion de documents scientifiques de niveau recherche, publiés ou non, émanant des établissements d'enseignement et de recherche français ou étrangers, des laboratoires publics ou privés.

Comparison of Two Fast Pressure Sensitive Paints: Measurements of an Oscillating Shock in a Transonic Flow

Walter H. Beck¹, Christian Klein² and Ulrich Henne³

German Aerospace Center DLR, Institute of Aerodynamics and Flow Technology, 37073 Göttingen, Germany

Marie-Claire Merienne⁴, Yves Le Sant⁵ and Pascal Molton⁶

Onera French Aerospace Lab, Aerodynamics, Aeroelasticity, Acoustics Department, 92190 Meudon, France

Abstract: The performance of two different PSP used at DLR and ONERA is compared by carrying out bench mark testing using the oft-studied configuration of an oscillating shock wave (up to 100 Hz) on a bump in the Mach 1.4 flow of the ONERA S8Ch wind tunnel. The shock is made to oscillate by rotating a cam with elliptical cross section, placed at a further downstream position, at frequencies of 15, 30 and 50 Hz. Both paint types are well known and much has been published on their use: the ONERA PSP is a Ruthenium complex $\text{Ru}(\text{dpp})_3\text{Cl}_2$ placed as a thin layer on an anodized aluminum substrate, while the DLR PSP is a Platinum complex PtTFPP on a base coating containing TiO_2 particles. S8 run conditions were held constant, and separate test run series were carried out with each paint. Instationary calibration was also carried out using a special test rig. Fourier analyses of the PSP results in S8 enabled a semi-quantitative comparison of the time response of both paints. This is the first published attempt (to the authors' knowledge) of carrying out a side-by-side comparison of the characteristics of these two paints on such a flow configuration in a wind tunnel. Particular emphasis is placed on their handling properties and, above all, their time responses.

I. Introduction

There has been increased interest in recent years in the measurement of fast processes (instationary or unsteady or periodic) in aerodynamic flows. Test models coated with Pressure (or Temperature) Sensitive Paints (PSP or TSP) have been used in the DLR and ONERA over recent years in various wind tunnels (WT) to measure pressures/temperatures and/or their changes on the model surface - see [1-9].

In recent years, an increased interest ([10-14], and for TSP: [15-17]) in the study of instationary flow physical phenomena (transition, turbulence, separation, heat transfer) has led to a requirement for fast acquisition systems: high speed cameras, high power (pulsed) LED's and, above all, paints with sufficiently fast response times to enable these instationary or short-duration phenomena to be captured quantitatively and faithfully. These techniques have kept pace with these requirements through: (1) improvements in and further development of paint formulations (both the luminophore itself, as well as its substrate and/or binder); (2) the availability in recent times of new high power light sources in the blue/UV wavelength regions (especially high power LED's); (3) the advent of high speed (usually CMOS) cameras which can capture full-chip images up to 20 kHz framing rates. A good overview of recent work on unsteady PSP measurements at Tohoku University in Japan has been given by Asai [18].

Typically, there are two major classes of PSP which have been used at DLR and ONERA to study these fast processes: (1) a Ruthenium complex salt $\text{Ru}(\text{dpp})_3\text{Cl}_2$ placed as a thin layer on an anodized aluminum substrate [19]; and (2) a Platinum complex PtTFPP on a base coating containing TiO_2 particles (see earlier DLR publications listed above). The former approach has been pursued by the team at ONERA, the latter by DLR: the two approaches will be referred to in this paper as

¹ Research Scientist, AIAA Associate Fellow, Experimental Methods Department, walter.beck@dlr.de

² Research Scientist, AIAA Associate Fellow, Experimental Methods Department, christian.klein@dlr.de

³ Research Scientist, Experimental Methods Department, ulrich.henne@dlr.de

⁴ Research Scientist, marie-claire.merienne@onera.fr

⁵ Research Scientist, yves.le_sant@onera.fr

⁶ Research Scientist, pascal.molton@onera.fr

uPSP (ONERA method) and iPSP (DLR method). The aim of this work is to devise a suitable test bed which would enable a comparison of the performance of uPSP and iPSP. This chosen test bed will now be described.

In the 1980's there was considerable interest in the problem of aircraft buffeting, leading to a search for a suitable wind tunnel configuration for studying and understanding the interaction between a shock impinging on a (perhaps instationary) boundary layer. In order to reproduce and simulate this phenomenon in a wind tunnel with a test model simpler than that of an aircraft or aircraft wing, Delery [20] devised an experiment where a bump was placed on the floor of a test section in a tunnel with a Ma 1.4 flow (the ONERA S8Ch wind tunnel); the conditions were so chosen as to provide nearly choked flow, leading to formation of a shock on the downstream part of the bump, which in turn interacts with the boundary layer on the test section floor. The position of this shock is critically dependent on the run conditions, especially on the degree of blockage. In his experiment, Delery changed this blockage by placing a cam with elliptical cross section in a position downstream of the bump, whereby maximal/minimal blockage was attained with the long elliptical cam axis being in vertical/horizontal directions, respectively, leading to a shock at different positions on the bump (vertical = more blocked = shock further upstream; horizontal = less blocked = further downstream). When this cam was rotated rapidly, the shock oscillated at twice this rate between these two extreme upstream/downstream shock locations. Many experiments using this test arrangement have been carried out at ONERA over the last 30 - 40 years, so that a large amount of data and experience is available, meaning that one can be very comfortable with generating reproducibly the right conditions for carrying out these paint comparison measurements [21, 22].

This configuration was chosen as the unsteady flow test bed for comparison of the two paints: the test section floor and bump were coated with the paints for measurements in separate experiments, and the rapidly changing pressures on the surface, arising from the shock/boundary layer interactions, were recorded by placing a camera above the test section, looking down onto the floor and bump. This is shown in Fig. 1, where a schematic description of the setup is given, showing the bump, the cam, the coated surface, the camera position and the two extreme upstream and downstream shock positions. Inset is a Schlieren image taken from the side with cam rotation rate of 15 Hz and taken just before the actual PSP measurement itself; to be seen are the bump on the floor, the (bifurcated) shock on this bump and the turbulent boundary layer downstream of the shock lambda foot (see more on this later).

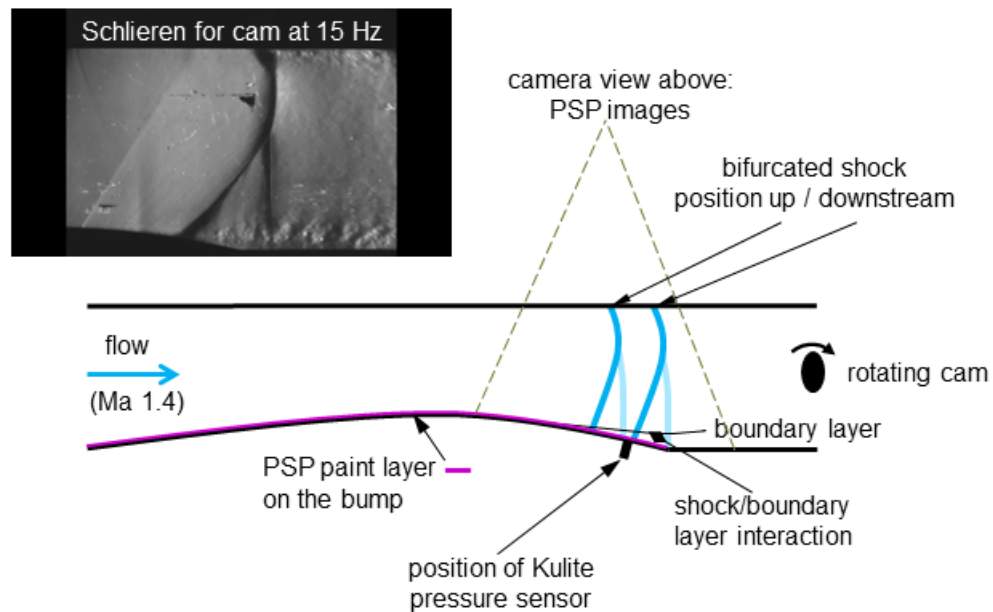


Fig.1 Schematic showing physical concepts and rationale behind the experiment. Inset: Schlieren result, cam 15 Hz.

Using this convenient test bed, experiments were carried out all at the (nominally) same wind tunnel conditions (Ma 1.4), and with the cam either stationary in vertical or horizontal axis orientations, or rotating at various speeds (15, 35 and 50 Hz, leading to shock oscillations of 30, 70 and 100 Hz, respectively). The performance of the paints was compared, with tests in both the wind tunnel and in an instationary test rig at DLR. Fourier analyses were carried out, both on the PSP images and on the pressure measured using a pressure sensor placed on the floor. Finally, a table was compiled comparing the

characteristics of both paints; this includes performance, speed, intensity, sensitivity, handling, aging, roughness, durability, test model requirements, and others.

II. Experimental setup

The same test model (the bump on the floor) could be coated with the two paints and measurements carried out (in separate tests) involving a Mach 1.4 flow over a bump on the floor of the ONERA Transonic Wind Tunnel S8Ch [23, 24]. As shown in Fig. 1, in passing over the constriction (viz. the bump) in the test section, the Ma 1.4 flow becomes nearly choked, leading to the formation of a shock downstream of the highest point of the bump (essentially a throat). (The interaction of this shock with the test section boundary layer also leads to its bifurcation, as shown in the sketch inset.) As stated before, the position of the shock is critically dependent on the amount of blockage (choking) of the flow; as this blockage increases or decreases, the shock moves in an upstream or downstream direction, respectively. (Its positioning at the highest point of the bump would correspond to the well-known fully choked flow in nozzles.)

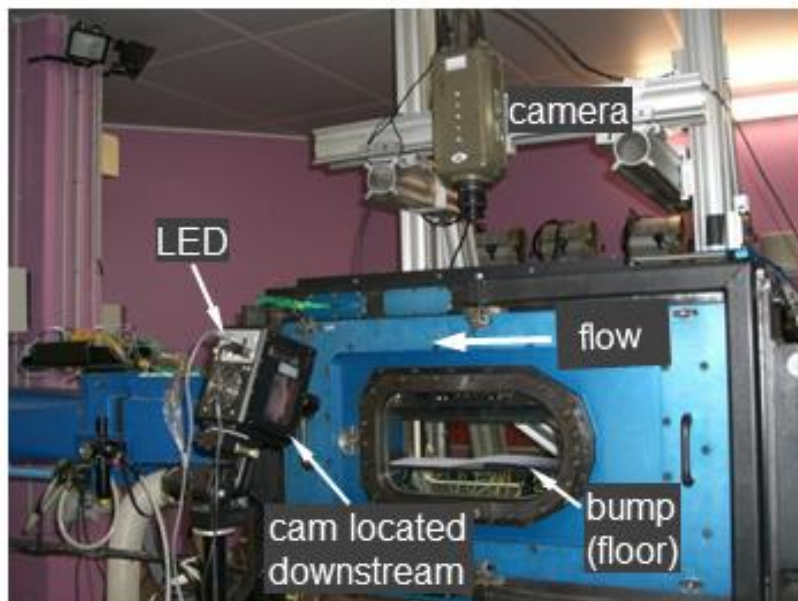


Fig.2 Experimental setup in S8 test section.

A cam with an elliptical cross section is placed downstream of the bump; in non-rotating mode, the vertical and horizontal positions lead to an additional blockage, this being greater for the vertical position, with the result that the shock is also situated a small amount further upstream compared to the horizontal orientation; this is shown in Fig. 1 sketch, which shows the shock position for both vertical and horizontal orientations of the cam. The cam rotation leads to an oscillatory movement of the shock between these two extrema positions. This movement leads to a periodic increase and decrease in pressure on the test section (bump) floor, its rate of change being dependent on the cam rotation speed. This periodic pressure change thus provides a good test bed for comparing the performance of uPSP and iPSP formulations.

Pressure was measured on the floor using a Kulite pressure sensor at the position shown in Fig. 1, and by the two different PSP (in separate tests) coated on the floor, shown in pink in Fig. 1. The PSP was irradiated from the side using a Hardsoft IL 106X LED in CW mode (excitation wavelengths were 400 nm and 460 nm for iPSP and uPSP, respectively), and images of paint fluorescence at wavelengths 650 nm were captured by a Phantom v710 camera (1280 x 800 pixels) situated above the test section, see Fig. 2 for photo of setup. Tests were done with the cam: (i) without rotation, fixed with its long axis in both vertical and horizontal orientations; and (ii) with rotation at frequencies of 15, 35 and 50 Hz, leading to shock oscillation frequencies of 30, 70 and 100 Hz, respectively. Camera acquisition rates were between 1080 and 3600 images/s, depending on cam rotation speed, with corresponding exposure times between 920 and 270 μ s, respectively. Small regions of interest (ROI) of size 10 x 30 mm (see Fig. 3), lying directly adjacent to the Kulite pressure sensor locations, were

identified, and the average PSP pressures therein used for a comparison with the adjacent Kulite pressure values. To be seen in Fig. 3 are the bounds of the cropped images used for later Fourier analyses; this is also shown in Fig. 4, which is a photo looking down onto the test section floor and bump, taken from above, with the view as seen by the fluorescence recording camera, which is also situated above (see Fig. 2). Figs. 3 and 4 show the bounds of the cropped image, and the extrema of shock oscillation location at 15 Hz cam rotation rate (dashed lines in Fig. 4).

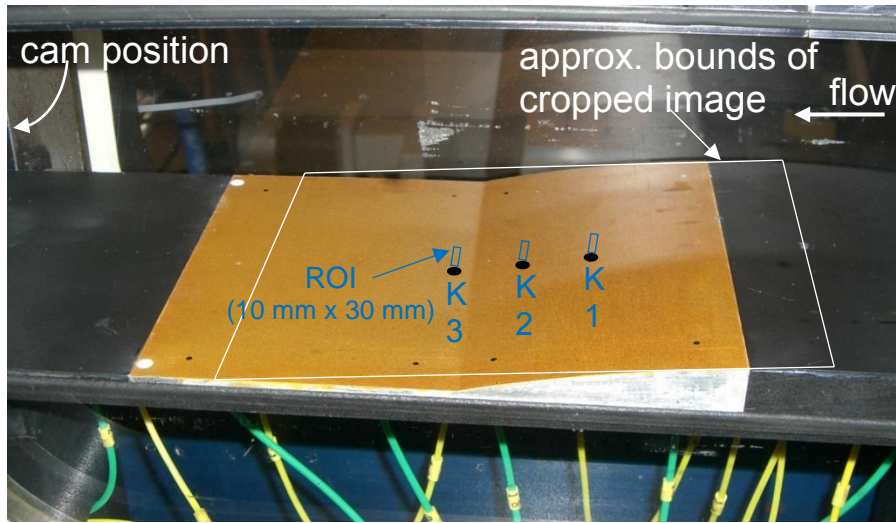


Fig.3 View of the coated insert (here for uPSP) on the floor and at the start of the bump. Also shown are: positions of the three Kulite pressure sensors (results from only sensor K2 will be shown later); cam is positioned further downstream (out of picture); white rectangle shows the bounds of the cropped PSP image used for analysis; regions of interest ROI, used to obtain an average pressure for comparison with pressure measured by the adjacent sensor.

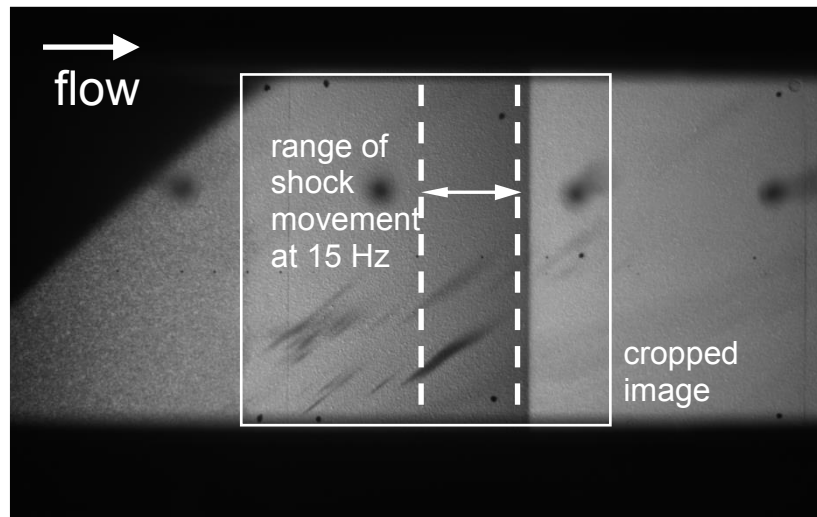


Fig.4 Photo looking onto the test section floor and bump, taken from above, with the view as seen by the fluorescence recording camera, also situated above (see Fig. 2). Bounds of the cropped image are shown. The extrema of shock oscillation location are also shown as dashed lines.

Stationary calibration of the uPSP and iPSP (for results see Section III.A.1), carried out at both DLR and ONERA were used to convert the captured fluorescence image intensities to 2D pressure fields on the bump. Schlieren images (an example

with the cam rotating at 15 Hz has already been shown in Fig. 1) were also recorded just prior to the PSP recordings to provide a check on proper tunnel operation, correct shock position and oscillation.

Since the time response of these paints is considered their most important attribute for use in measuring unsteady processes, samples of both were tested in the DLR instationary test rig; here a pressure chamber, containing coated sample and Endevco pressure sensor, and equipped with a window (via which the PSP sample could be irradiated and its fluorescence recorded), has at one end a movable membrane (as in a loudspeaker), which can be brought to vibrate using a plunger-type actuator, hence producing (small) pressure oscillations in the chamber [25]. Fluorescence of the paint was measured with a photodiode with a very fast time response ($<10 \mu\text{s}$). The setup is shown in Fig. 5. A Fourier analysis of the photomultiplier signals and the Kulite traces leads to the determination of a transfer function $H(\omega) = F_{\text{out}}(\omega) / F_{\text{in}}(\omega)$ (shown also in Fig. 5), which provides information on the offset, amplitude and phase relationships between the two measurement methods PSP and Kulite sensor (this latter has a very fast time response).

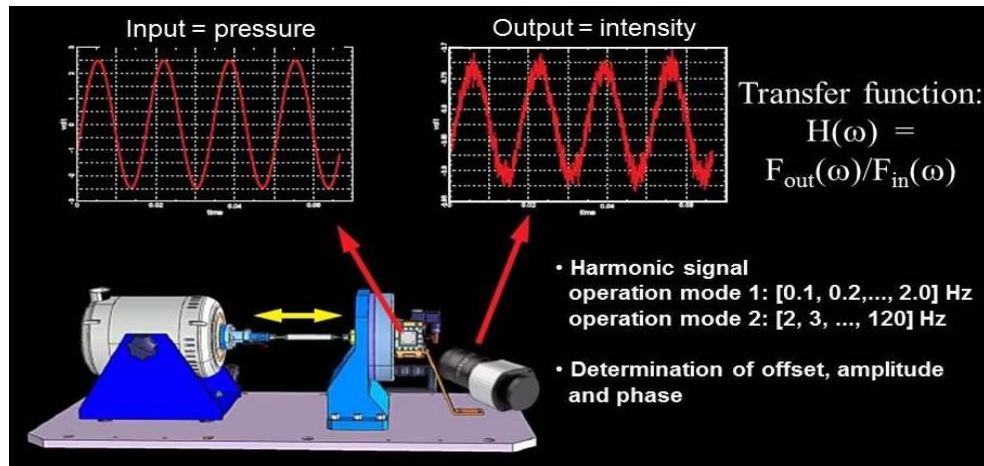


Fig.5 The DLR instationary pressure calibration test rig, showing the plunger actuator, vibrating membrane housing, sample chamber with window and photomultiplier. For further description, see text.

A pixel-by-pixel Fourier analysis of several 2D PSP pressure images obtained from the wind tunnel test was also carried out. This led to a series of RMS images (2D spatial plots) at several frequency bands, showing the correlation (RMS value) for each particular frequency at various positions on the 2D plot. See Section III.D.

III. Results and discussion

A. PSP calibration

1. Stationary calibration

The stationary calibration test rigs are sealed chambers containing a sample Al coupon coated with the paints; pressure and temperatures in the chamber were varied from 10 – 140 kPa and 10 – 30°C, respectively. Results are shown in Fig. 6: for both iPSP (upper) and uPSP (lower), inverse intensity values I_{ref}/I (where I_{ref} corresponds to intensities at $T = 20 \text{ C}$ and $P = 100 \text{ kPa}$) are plotted as a function of pressure P (left) and temperature T (right). The measured gradients (paint responses to P and T) dI/dP and dI/dT are also noted in the figure. Obviously one would prefer a large dI/dP and low dI/dT for the PSP measurements here. The results show that dI/dP is larger for iPSP, which, unfortunately, also has a higher dI/dT ; this would normally be undesirable, only that in these experiments the temperature changes on the model surface were not large so that temperature corrections were not needed.

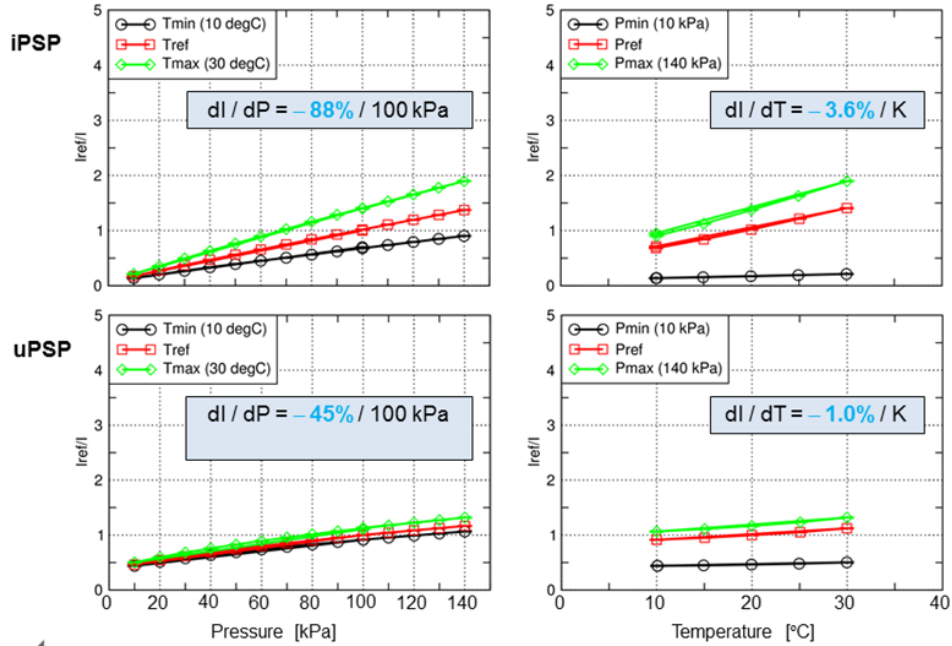


Fig.6 Calibration results for iPSP and uPSP at various pressures P and temperatures T. Pressure (dI/dP) and temperature (dI/dT) sensitivities are also shown.

2. Instationary calibration

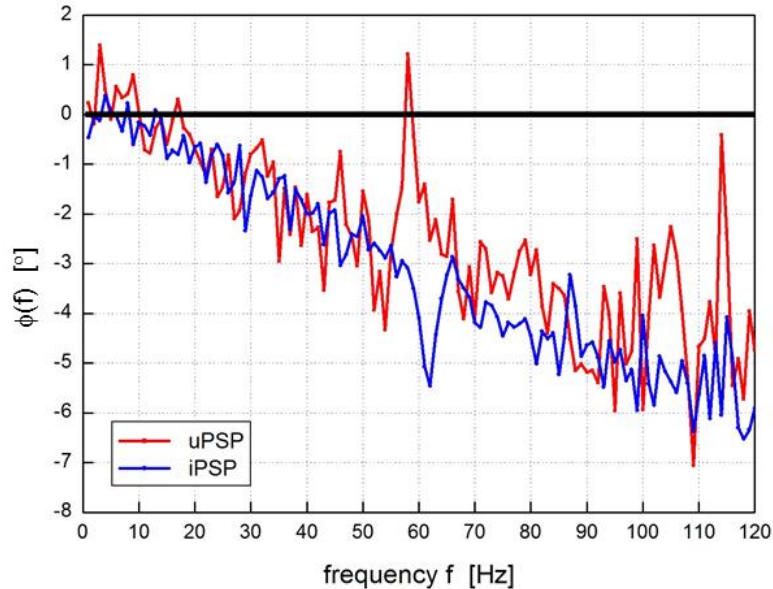


Fig. 7 Comparison of phase shifts for uPSP and iPSP, measured in the DLR instationary pressure calibration test rig.

Instationary calibration was carried out at frequencies up to 120 Hz. A result is shown in Fig. 7 for the phase shift $\phi(f)$ [°] of the two points relative to the pressure sensor results, plotted as a function of frequency f [Hz]. One sees here a continuously increasing phase lag for both points as frequency is increased, reaching about -5° at 120 Hz. There is no great difference in behavior between the two points, and in fact up to 50 Hz the results are the same; at frequencies above 50 Hz

the uPSP phase lag is slightly less than with iPSP, but this is to some extent masked by the larger oscillations in the uPSP plot. A comparison of the amplitudes for the power spectra showed that uPSP had no losses (unchanging amplitude) up to 120 Hz, whereas for iPSP the amplitude dropped. No tests were done at higher frequencies. This result alone is not conclusive: more about the paint time responses can be learnt from analyses of the results from the wind tunnel test itself, where an analysis up to higher frequencies (600 Hz) was carried out. This will be discussed in Section III.D.

B. Raw images from iPSP and uPSP (including Schlieren)

Sample raw fluorescence images for both iPSP and uPSP with the cam (long) axis fixed in horizontal and vertical directions are shown in Fig. 8. Since the cam is non-rotating (0 Hz), the shock remains on average in the one location; this is, however, obviously different for these two cam positions, due to the different degrees of blockage obtained (greater for vertical), as discussed earlier. A film of the various images captured over time shows that the shock is anything but fully stationary; although its average position does not change, the shock front is seen to wobble and distort. This can be seen for both cam positions and both paints, but is seen to be more pronounced for the vertical cam location, where the blockage is greater, and where the shock/boundary layer interactions are expected to be greater.

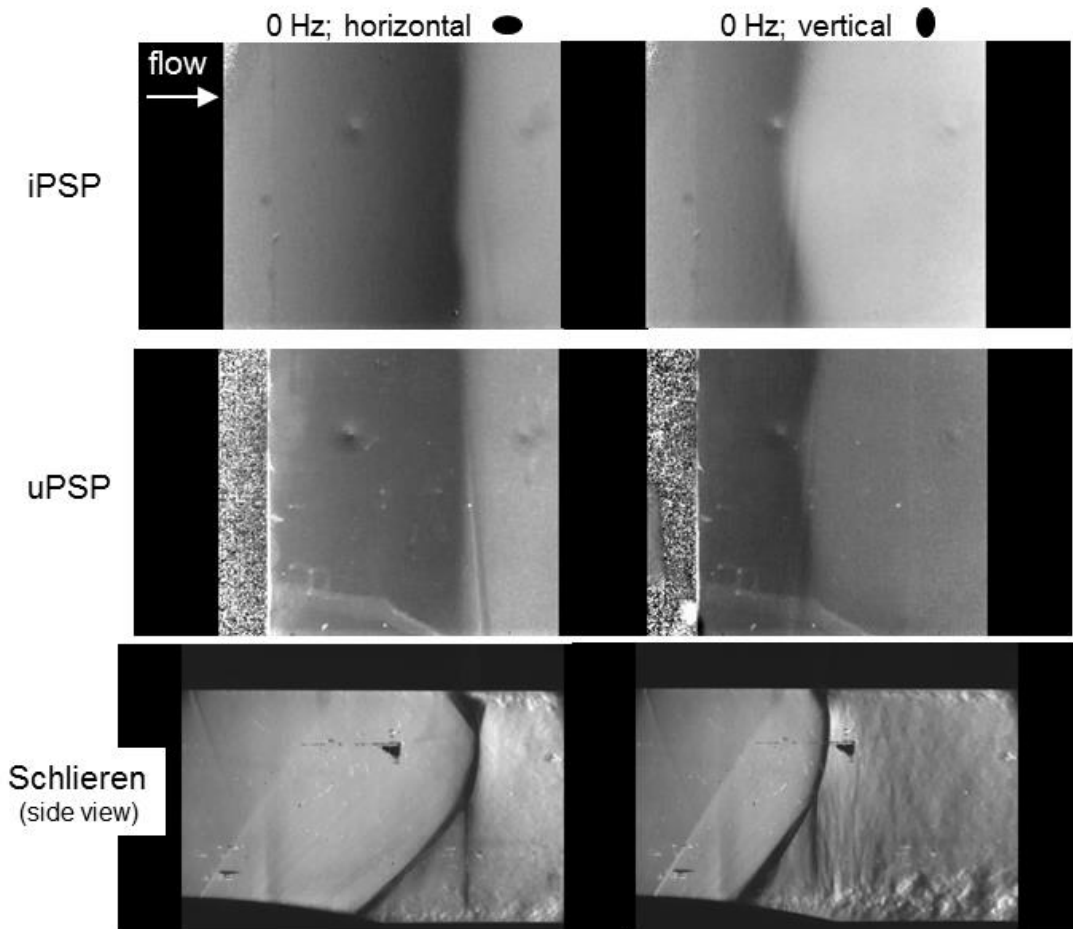


Fig. 8 PSP raw images for both paints iPSP and uPSP (as seen with the camera from above), with cam in horizontal and vertical positions. For comparison, Schlieren images taken immediately prior to the PSP measurements are also shown (side view) – here the bifurcated shock and (turbulent) boundary layer can be clearly seen.

Fig. 8 also shows Schlieren images for the two cam axis locations. In both cases the strong bifurcation of the shock, leading to a pronounced lambda foot, can clearly be seen. Furthermore, the test section floor boundary layer after the lambda foot on the bump can be seen to grow markedly in size and become turbulent. Again, as expected, this effect is greater for the vertical cam case.

C. Comparison: PSP with Kulite pressure sensor results

Fig. 9 shows a comparison of pressure measurements on the bump in the Ma 1.4 flow from the Kulite pressure sensor K2 (red trace) and iPSP and uPSP (black/blue traces); for the latter measurements, the small interrogation region (ROI) adjacent to the Kulite position, as discussed before, was used to obtain an average pressure for PSP over this ROI. Measurements with three cam frequencies are shown: at 15, 35 and 50 Hz. It can be seen in the figure that both PSP methods can faithfully track the *change* of pressure, even at the maximum shock oscillation rate of 100 Hz (2 x 50 Hz cam frequency). There is, however, also a small consistent pressure *offset* between Kulite and PSP results; this is a known phenomenon in quantitative PSP measurements. (Note that the customary offset corrections have not been applied here.) Note also that, unfortunately, and inexplicably, flow conditions were not identical for the iPSP and uPSP run series – the shock location was different – so that the pressure amplitudes for these were also different, as can be seen in Fig. 9. This difference in shock location could be inferred by a comparison of the Schlieren results, and is further exemplified by the Fourier RMS plots, to be discussed in a later section (see Fig. 13 in Section III.D.2).

In spite of differences in pressure levels (no offset correction), the time correlation between the Kulite and PSP results is seen to be very good, even at the highest cam rotation rate of 50 Hz. From these results in Fig. 9 there does not seem to be a large difference in response of either of the paints – both seem to match the Kulite results quite well. However, the Fourier analyses carried out, to be discussed later (Section III. D.1), do show a difference, especially noticeable at higher frequencies where overtones of the fundamental oscillation frequencies f_{osc} ($n \times f_{osc}$, $n = 1, 2, 3, \dots$) can be seen – see Section III.D.1.

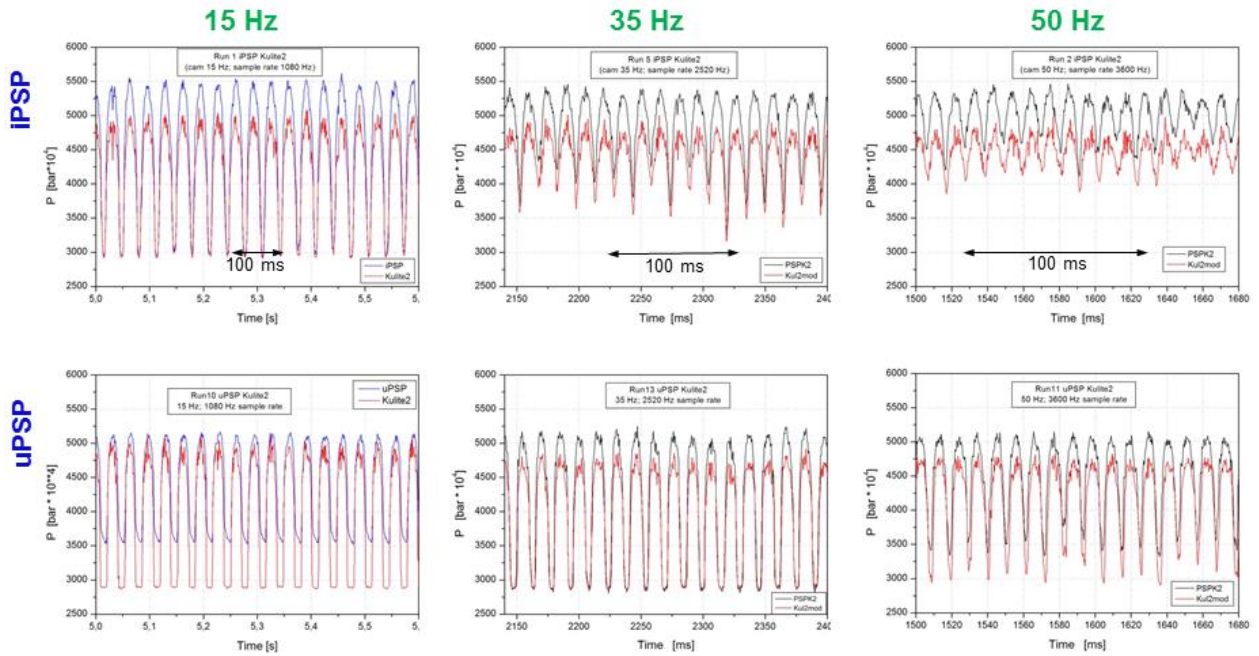


Fig. 9 Comparison of pressure measurements from Kulite sensor K2 (red) and PSP (blue/black) in the Ma 1.4 flow for iPSP and uPSP at cam frequencies of 15, 35 and 50 Hz (30, 70 and 100 shock oscillation frequency).

D. Spectral analysis

A brief overview of the data processing follows. The ratio between the wind-off image, also called the reference image, and the wind-on image is formed. Due to possible model movement during wind-on, it is necessary to align the two sets of images prior to computing the ratio and applying the calibration law: this is done with Onera in-house software (AFIX2) for optical measurement methods which has been further developed and refined over many years [3]. New tools have been included for unsteady applications such as phase averaging and spectral analysis. The latest development is the implementation of the GPU (Graphic Processor Unit), which enables an efficient management of large numbers of images and a dramatic reduction of the computing time of at least one order of magnitude. The benefits of this approach have been amply demonstrated with a GPU-based PIV code [26].

Fourier analyses of the PSP results are expected to provide further quantitative details of the time response of the paints. The camera (and certainly Kulite – not shown here) recording rates were sufficiently high (as given by the Nyquist criterion) to enable an analysis of frequencies covering several overtones of the respective fundamental frequencies, here up to at least 700 Hz (from $n \times f_{\text{osc}}$, for $n = 7$ and $f_{\text{osc}} = 100$ Hz). The analyses were carried out in two different ways, to be discussed in this section. 1. *Power spectral density line plots*: the average pressures in the ROI near sensor K2 (see Fig. 3) for all images over time from both iPSP and uPSP were analyzed using an efficient FFT algorithm [27] to obtain spectral power line plots as a function of frequency. 2. *Power spectral density maps*: here all PSP images over time were analyzed pixel-by-pixel, again using the FFT algorithm, giving a PSD (power spectral density) value at each pixel location. The final result is a 2D map with spatial coordinates corresponding to those of the cutout shown in Figs. 3, 4 and 8, and with spectral power values shown for each pixel, presented in a color map in units of kPa^2/Hz .

1. Power spectral density line plots

The FFT analysis of the ROI led to power spectral plots PSD [$\text{Pa}^2 \text{Hz}^{-1}$] plotted as a function of frequency f [Hz]; these spectra for both paints are compared in Figs. 10 - 12.

Fig.10 shows a power spectral plot for a cam frequency of 15 Hz (shock 30 Hz), where the iPSP and uPSP results are shown as black and blue traces, respectively. As expected, both iPSP and uPSP have the strongest peak at the fundamental frequency $f_{\text{osc}} = 30$ Hz. Although several overtones up to $n = 7$ can be clearly seen for both paints, only the uPSP has a peak at higher frequencies – here overtones up to at least $n = 9$ are discernible, and there is even a hint of a peak at $n = 11$. From this result one can infer that uPSP has the better time response.

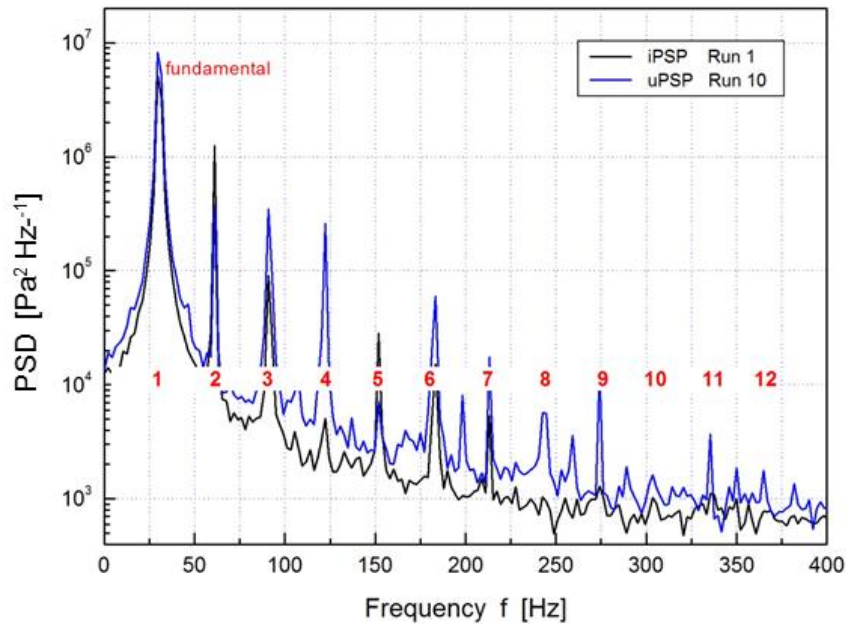


Fig. 10 Comparison of power spectra from PSP measurements (ROI) for uPSP and iPSP (cam 15 Hz, $f_{\text{osc}} = 30$ Hz). Fundamental at 30 Hz and overtones up to $n = 12$ are indicated.

A further comparison is provided by the power spectra for $f_{\text{osc}} = 100$ Hz – see Fig. 11. Here overtones at higher frequencies than at 30 Hz are to be expected; if they are indeed at all present. Fig. 11 shows clear peaks for uPSP up to overtone $n = 6$, whereas for iPSP the peak at $n = 4$ is the last which can be unequivocally assigned.

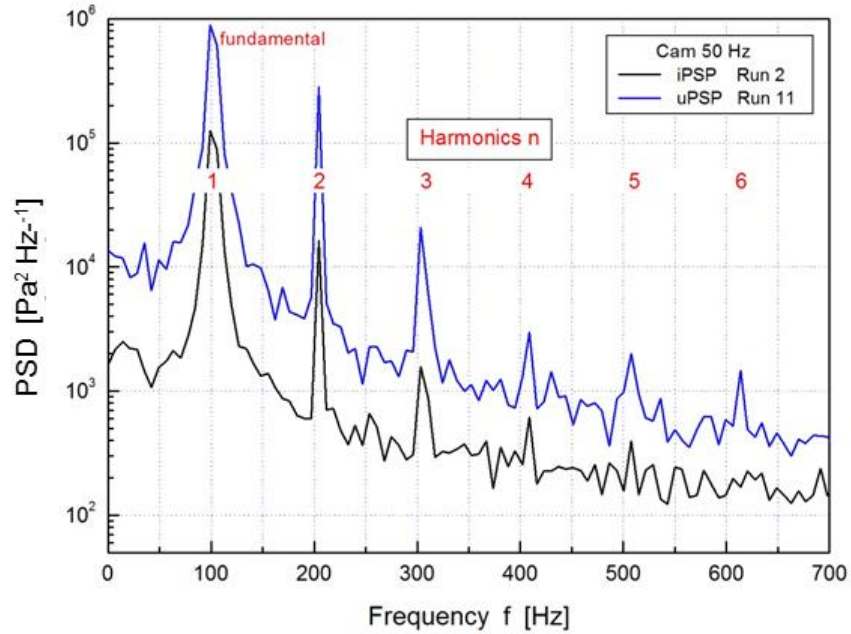


Fig. 11 Comparison of power spectra from measurements (in ROI) for uPSP and iPSP (cam 50 Hz, $f_{osc} = 100$ Hz).

To make a comparison of the time response of the two paints easier, the *relative* power densities (in effect, the ratios of the areas under the curves in Fig. 11) for each harmonic n , namely $PSD(n)^{uPSP} / PSD(n)^{iPSP}$, are plotted for both paints against frequency in Fig. 12 (note that the ordinate is a logarithmic scale). The result at 600 Hz clearly emphasizes the conclusion discussed before that the uPSP has a faster response, even though their behavior up to 500 Hz is quite similar.

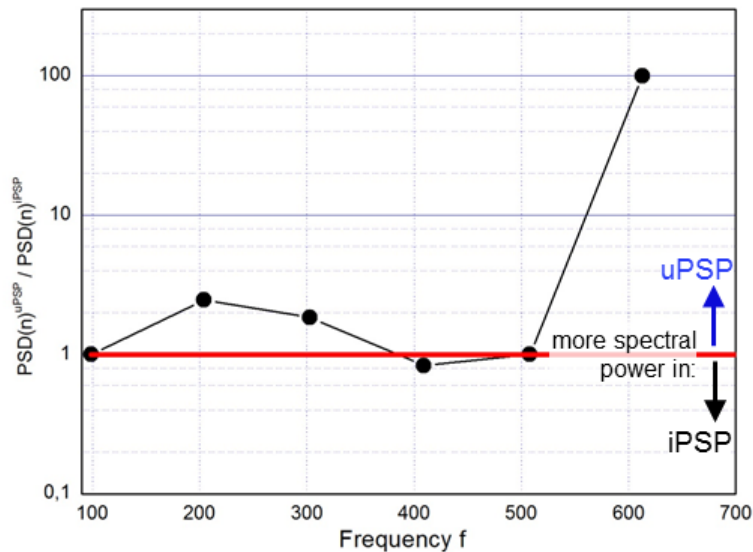


Fig. 12 Relative spectral powers for uPSP and iPSP (cam 50 Hz, $f_{osc} = 100$ Hz).

Plots of PSD for PSP and the Kulite sensors for $f_{osc} = 30$ Hz and 100 Hz are presented in Fig. 13. All PSD have been calculated with the same number of data points at the same sampling rate, thus enabling a comparison of the noise levels and cut-off frequencies. Strong peaks at the fundamental frequencies (50 and 100 Hz) are clearly visible, as expected, as well as

the higher order harmonics. As already seen for the pressure results shown in the plots pressure vs time in Fig. 9, the shift in amplitude (PSD) between the Kulite and PSP results can also be seen here, being especially pronounced for $f_{osc} = 100$ Hz.

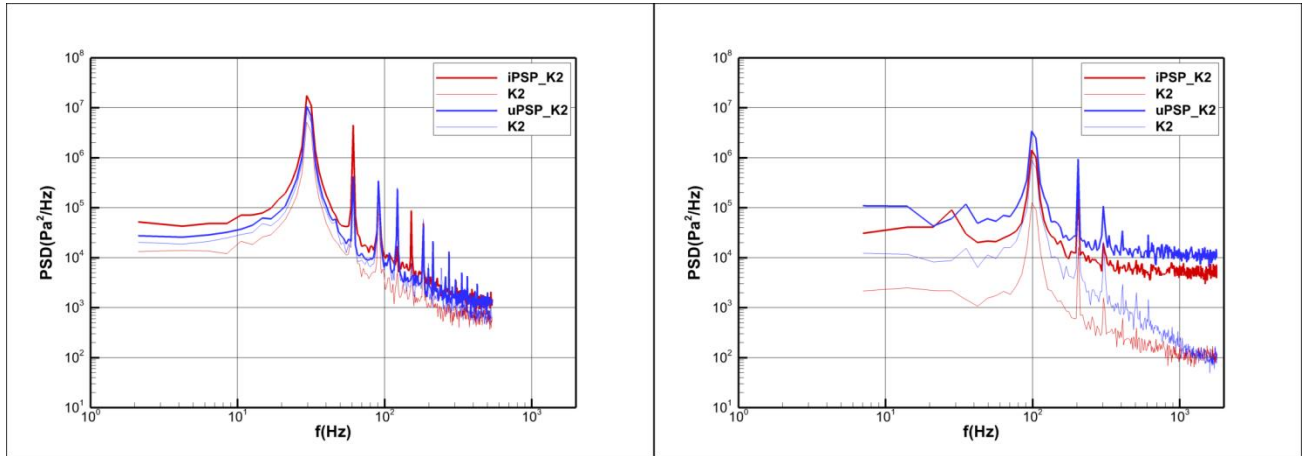


Figure 13: Comparison of PSD for iPSP/uPSP (bold lines) with Kulite sensor K2 (thin lines) at the same position for $f_{osc} = 30$ Hz (left) and 100Hz (right).

2. Power spectral density images

The RMS plots for the two runs at $f_{osc} = 100$ and 30 Hz (cam rotation frequencies of 50 and 15 Hz, respectively) are shown for both iPSP and uPSP in Fig. 14. The spatial coordinates correspond to those of the cutout (cropped region) discussed before (see Figs. 3, 4 and 8): in this plan view the edge of the insert can be discerned clearly to the left in each image (also labelled). The end of the bump is also shown. Each pixel value in kPa (see color bar) provides a value of the pressure variation at that pixel location. As already mentioned, the flow conditions are not identical for the two paints; the maximum pressure variations at 100 Hz for iPSP and uPSP are 10 kPa and 7 kPa, respectively.

As expected, the RMS value is larger for those regions on the bump where the shock oscillation is actually occurring; these maps hence also give a good measure of the spatial extent over which this shock oscillation occurs.

There is obviously a whole family of plots corresponding to various frequencies for each of the two runs. Fig. 15 shows 12 images of a Fourier analysis for the iPSP run only and with a *nominal* cam frequency of 15 Hz (hence *nominally* $f_{osc} = 30$ Hz). (Obviously the cam frequency was not exactly 15 Hz; 29.5 Hz corresponds to the actual *measured* frequency f_{osc} .) The 12 maps represent results for frequencies ranging from 2.1 in steps of about 2.1 Hz up to 29.5 Hz. Also note that the color bar for the last map at 29.5 Hz has been scaled differently to the other 11 maps; the scaling factor is 500! As expected, the energy is considerably smaller (*viz.* O. 500) for frequencies below the fundamental at 29.5 Hz.

Note furthermore, as mentioned earlier, that the images for iPSP and uPSP in Fig. 14 show different shock locations and also larger values in RMS value for iPSP than for uPSP; the tests had been supposedly carried out under identical run conditions, but the shocks were nevertheless inexplicably in different locations. This is clarified in Fig. 15, where the map for 29.5 Hz (last image) shows the extent of shock movement for iPSP (white vertical lines) and for uPSP (black vertical lines) – the two regions do not overlap. This does not, however, in any way influence or detract from the conclusions regarding the relative time responses of the two paints.

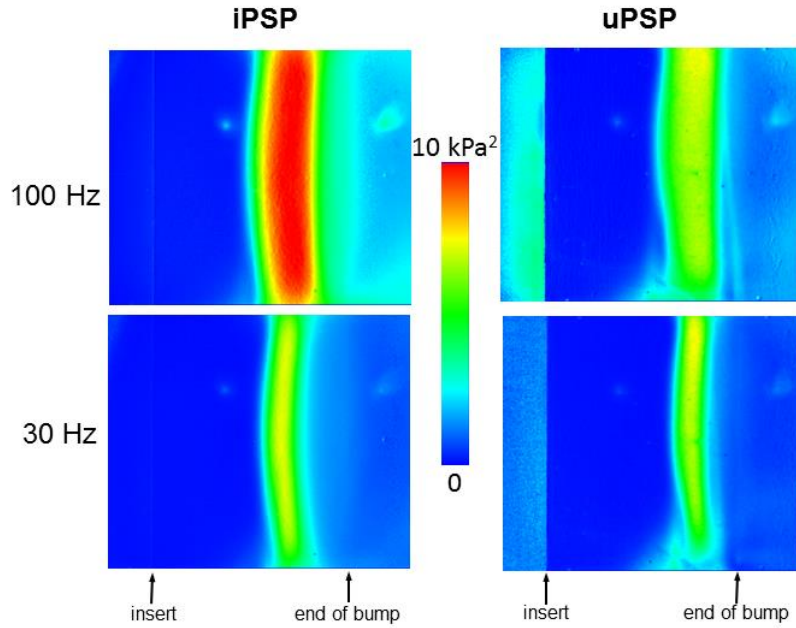


Fig. 14 RMS plots on the test section floor and bump surfaces for both iPSP and uPSP and for cam frequencies of 50 and 15 Hz ($f_{osc} = 100$ and 30 Hz, respectively). View is from the top onto the floor and bump. Top and lower boundaries of the images correspond to side wall positions; in other words, one sees the result over the whole test section width. Flow is from left to right.

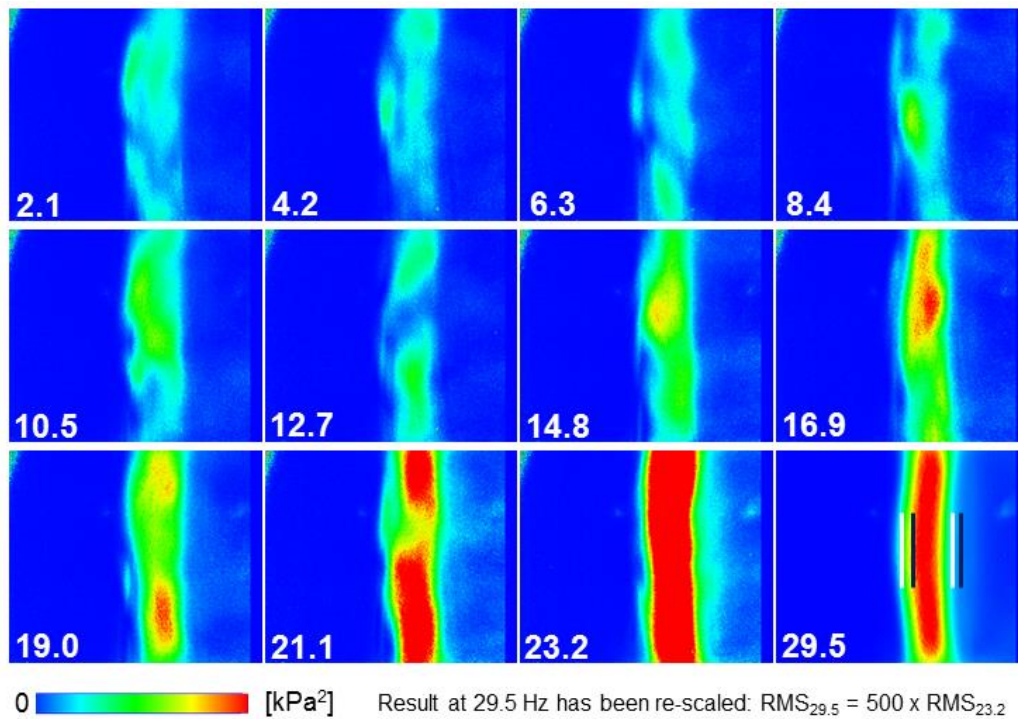


Fig. 15 PSD plots on the test section floor and bump surfaces for iPSP and for cam frequency 15 Hz, showing Fourier frequencies in 12 maps with frequencies from 2.1 up to 29.5 Hz. Note that f_{osc} is *nominally* 30 Hz; measured was actually 29.5 Hz (cam rotation was less than 15 Hz). The map at 29.5 Hz shows the bounds of shock movement for iPSP and uPSP as white and black vertical lines, respectively. See Fig. 13 for further description.

IV. Comparison of paint characteristics

Many criteria need to be considered in comparing the performance of uPSP and iPSP. The discussion so far has been centered on mainly the paint time response, viz. its ability to track faithfully fast changing pressures. This is clearly the major requirement. This, but also other criteria, are listed in the following Table 1 showing a comparison of uPSP with iPSP. There has been no discussion in this paper of the other paint properties and characteristics listed in the table (handling, time, durability, humidity, removal, test model size/geometry, surface roughness, photodegradation, in situ application, image quality, fluorescence intensity, pressure and temperature sensitivity); they are presented *per se* for the sake of completeness and without further discussion. Note that the interpretations and assessments are based on this one-off study; some properties such as fluorescence intensity and pressure/temperature sensitivities may vary due to differences in the method of paint preparation and coating. The fields in the table with green backgrounds show where the one paint has some advantage over the other. In summary, it can be said that the paints have both advantages and disadvantages; which paint is to be preferred depends to a large extent on the application.

Characteristic	iPSP	uPSP
ease of application	spraying two layers; easy	electrolysis, then dipping; less easy
preparation time	1 - 2 days	1 - 2 days
durability : handling; wind-on; dust	good; good; poor	good; good; fair
effect of humidity on paint: life; sensitivity	good; reduced	fair; reduced
paint removal ; ease of; surface quality	easy (paint stripper); as new	not easy (Al ₂ O ₃ removed with NaOH); fair
model : size; re-use; material	unlimited; yes; any	limited by bath size; maybe; only Al
surface roughness R _a [μm]	2 (but 0.5 can now be achieved)	0.5
photodegradation	more sensitive	less sensitive (0.03% / minute)
complex 3D geometries	yes (spraying)	difficult (electrolysis difficult)
<i>in situ</i> application on instrumented models	yes	no (electrolysis needs bath)
image quality	very good	good (if dipping is good)
time response (phase shift φ)	quite good up to 120 Hz (φ < 5°) (no peaks > ~220 Hz)	good up to 120 Hz (φ < 5°) (peaks up to ~350 Hz)
signal intensity	good	very good
pressure sensitivity dI/dP [% / 100 kPa]	-88	-46
temperature sensitivity dI/dT [% / K]	-3.6	-1.0

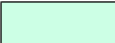
 where one paint may have some advantage over the other (in these tests)

Table 1 Comparison of various characteristics and properties of uPSP and iPSP. Green backgrounds show where the one paint can be considered to have some advantage over the other.

V. Summary and conclusions

Various characteristics of iPSP and uPSP have been compared in a bench mark test using an oscillating shock wave on a bump in the S8Ch wind tunnel with a Ma 1.4 flow. Measurements were compared with those of a Kulite sensor situated in the region of shock location, and Fourier analyses were carried out to compare their relative time responses. uPSP was shown to have a better time response than iPSP, where at frequencies above 100 Hz (overtones) the time response of the latter was not high enough to deliver any values. Various other characteristics, many property- and technique-related, are compared in a final table.

VI. Acknowledgements

We thank the following for their invaluable support: Marco Costantini (DLR): determination of iPSP material properties; Vlado Ondrus (University of Hohenheim): development of iPSP; Sebastian Dufhaus (now RWTH, Aachen): static calibration of iPSP /uPSP samples; Jean Delery (now retired): useful, helpful and informed discussions; Serge Ost (ONERA): technical test model support; Gilles Losfeld (ONERA): technical instrumentation support; Yves Carpels (ONERA): technical wind tunnel support.

VII. References

- [1] Engler, R. H., Klein, C. and Trinks, O. (2000), “Pressure sensitive paint systems for pressure distribution measurements in wind tunnels and turbomachines”, *Meas. Sci. Technol.* **11**, 1077 – 1085.
- [2] Klein, C., Engler, R. H., Henne, U. and Sachs, W. E. (2005), “Application of pressure-sensitive paint for determination of the pressure field and calculation of the forces and moments of models in a wind tunnel”, *Exp. Fluids* **39**, 475 – 483.
- [3] Le Sant, Y., Merienne, M. C. (2005), “Surface pressure measurements by using pressure-sensitive paints”, *Aerospace Science and Technology*, Vol 9, n°4, 180-299.
- [4] Merienne, M. C., Le Sant, Y. (2006), “Reliable PSP application and data processing at low speed flow conditions”, 25th AIAA Aerodynamic Measurement Technology and Ground Testing Conference, 5-8 June 2006, San Francisco, California, USA.
- [5] Streit, T., Horstmann, K. H., Schrauf, G., Hein, S., Fey, U., Egami, Y., Perraud, J., El Din, I. S., Cella, U. and Quest, J. (2011), “Complementary Numerical and Experimental Data Analysis of the ETW Telfona Pathfinder Wing Transition Tests”, 49th AIAA Aerospace Sciences Meeting, paper 2011-881, 4. – 7. January, 2011, Orlando, Florida, USA.
- [6] Klein, C., Henne, U., Sachs, W., Hoc, k S., Falk, N., Beifuss, U., Ondrus, V. and Schaber, S. (2013), “Pressure Measurement on Rotating Propeller Blades by means of Pressure-Sensitive Paint Lifetime Method”, 51st AIAA Aerospace Sciences Meeting, paper 2013-0483, 7. – 10. January, 2013, Grapevine, Texas, USA.
- [7] Fey, U., Klein, C., Ondrus, V., Loose, S. and Wagner, C. (2013), “Investigation of Reynolds Number Effects in High Speed Train Wind Tunnel Testing using Temperature-Sensitive Paint”, paper presented at 2nd International Symposium on Rail-Aerodynamics: Aerodynamics of Trains and Infrastructure, 15. – 17. May, 2013, Berlin, Germany.
- [8] Costantini, M., Risius, S. and Klein, C. (2014), “Experimental investigation of the effect of forward-facing steps on boundary layer transition”, presented at IUTAM, ABCM Symposium on Laminar Turbulent Transition, Rio de Janeiro, Brazil.
- [9] Klein, C., Henne, U., Sachs, W., Beifuss, U., Ondrus, V., Bruse, M., Lesjak, R. and Löhr, M. (2014), “Application of Carbon Nanotubes (CNT) and temperature-Sensitive Paint (TSP) for the Detection of Boundary Layer Transition”, 52nd AIAA Aerospace Sciences Meeting, paper 2014-1482, 13. – 17. January 2014, National Harbor, Maryland, USA.
- [10] Merienne, M. C., Le Sant, Y., Lebrun, F., Deleglise, B. and Sonnet, D. (2013), “Transonic buffeting investigation using unsteady pressure-sensitive-paint in a large wind tunnel”, 51st AIAA Aerospace Sciences Meeting, SciTech 2013, Paper 2013-1136, 7. – 10. January, 2013, Grapevine, Texas, USA.
- [11] Gregory, J. W., Sakaue, H., Liu, T. and Sullivan, J. P. (2014), “Fast Pressure-Sensitive Paint for Flow and Acoustic Diagnostics”, *Annual Review of Fluid Mechanics* **46**, 303-330.
- [12] Gardner, A. D., Klein, C., Sachs, W. E., Henne, U., Mai, H. and Richter, K. (2014), “Investigation of three-dimensional dynamic stall on an airfoil using fast-response pressure-sensitive paint”, *Exp. Fluids* **55**,1807.

- [13] Michou, Y., Deleglise, B., Lebrun, F., Scolan, E., Grivel, A., Steiger, R., Pugin, R., Merienne, M. C. and Le Sant, Y. (2015), "Development of a sol-gel based nanoporous unsteady pressure sensitive paint and validation in the large transonic ONERA's S2MA wind tunnel", AIAA Aviation, 31st AIAA Aerodynamic Measurement Technology and Ground Testing Conference, 22-26 June 2015, Dallas, TX, USA.
- [14] Scolan, E., Smadja, R., Weder, G., Voirin, G., Pugin, R., Michou, Y., Merienne, M. C., Lyonnet, M. and Winzer, A. (2016), "Integration of new sol-gel films into optical chemical sensors", 30th EuroSensors Conference, EUROSENSORS 2016, Budapest, Hungary.
- [15] Risius, S., Beck, W. H., Klein, C., Henne, U. and Wagner, A. (2017), "Determination of heat transfer into a wedge model in a hypersonic flow using Temperature-Sensitive Paint", *Exp. Fluids* **58:9**, paper 117 (13 pages).
- [16] Ozawa, H. (2016), "A highly temperature sensitive and ultra-fast response TSP (Temperature-Sensitive-Paints) for unsteady aerothermodynamics on shock-tube wall", 46th AIAA Fluid Dynamics Conference, AIAA AVIATION Forum, Paper AIAA 2016-3934.
- [17] Ozawa, H., Laurence, S. J., Martinez Schramm, J., Wagner, A. and Hannemann, K. (2015), "Fast-response temperature-sensitive-paint measurements on a hypersonic transition cone", *Exp. Fluids* **56(1)**, 1853.
- [18] Asai, K. and Daisuke, Y. (2011), "Unsteady PSP measurement in low-speed flow – overview of recent advancement at Tohoku University", 49th AIAA Aerospace Sciences Meeting, SciTech 2011, Paper 2011-847, 4. – 7. January, 2011, Orlando, Florida, USA.
- [19] Merienne, M. C., Coponet, D. and Luysen, J. M. (2012), "Transient pressure-sensitive paint investigation in a nozzle", *AIAA Journal*, Vol 50, 7, 1453-1461.
- [20] Delery, J. (1983), "Experimental investigation of turbulence properties in transonic shock/boundary layer interactions", *AIAA Journal* **21**, 180 – 185.
- [21] Merienne, M. C., Le Sant, Y., Ancelle, J. and Soulevant, D. (2004), "Unsteady pressure measurement instrumentation using anodized-aluminium PSP applied in a transonic wind tunnel", *Measurement Science and Technology* **15**, 2349 – 2360.
- [22] Merienne, M. C., Molton, P., Bur, R. and Le Sant, Y. (2015), "Pressure-sensitive paint application to an oscillating shock wave in a transonic flow", *AIAA Journal* **53**, 3208 – 3220.
- [23] Galli, A., Corbel, B. and Bur, R. (2005), "Control of forced shock-wave oscillations and separated boundary layer interaction", *Aerospace Science and Technology*, Vol. 9, 2005, pp. 653-660.
- [24] Sartor, F., Losfeld, G. and Bur, R. (2012), "PIV study on a shock-induced separation in a transonic flow", *Exp. Fluids*, Vol. 53, No 3, 2012, pp. 815-827.
- [25] Klein, C., Sachs, W. E., Henne, U. and Borby, J. (2010), "Determination of Transfer Function of Pressure-Sensitive Paint", 48th AIAA Aerospace Sciences Meeting Including the New Horizons Forum and Aerospace Exposition, 4 - 7 January 2010, Orlando, Florida, Paper AIAA 2010-309.
- [26] Champagnat, F., Plyer, A; Le Besnerais, G., Leclaire, B., Davoust, S. and Le Sant, Y. (2011) "Fast and accurate PIV computation using highly parallel iterative correlation maximization.", *Exp. Fluids* Vol 50, n°4 (2011): 1169-1182.
- [27] Brandon, L. D., Boyd, C. and Govindaraju, N. (2008); "Fast computation of general Fourier transforms on GPUs." Multimedia and Expo, 2008 IEEE International Conference on. IEEE, 2008.